

REPORT DOCUMENTATION PAGE			Form Approved OMB NO. 0704-0188		
<p>The public reporting burden for this collection of information is estimated to average 1 hour per response, including the time for reviewing instructions, searching existing data sources, gathering and maintaining the data needed, and completing and reviewing the collection of information. Send comments regarding this burden estimate or any other aspect of this collection of information, including suggestions for reducing this burden, to Washington Headquarters Services, Directorate for Information Operations and Reports, 1215 Jefferson Davis Highway, Suite 1204, Arlington VA, 22202-4302. Respondents should be aware that notwithstanding any other provision of law, no person shall be subject to any penalty for failing to comply with a collection of information if it does not display a currently valid OMB control number.</p> <p>PLEASE DO NOT RETURN YOUR FORM TO THE ABOVE ADDRESS.</p>					
1. REPORT DATE (DD-MM-YYYY)		2. REPORT TYPE		3. DATES COVERED (From - To)	
		New Reprint		-	
4. TITLE AND SUBTITLE			5a. CONTRACT NUMBER		
Gluing bifurcations in coupled spin torque nano-oscillators			W911NF-12-1-0283		
			5b. GRANT NUMBER		
			5c. PROGRAM ELEMENT NUMBER		
			611102		
6. AUTHORS			5d. PROJECT NUMBER		
Katherine Beauvais, Richard Shaffer, Antonio Palacios, Visarath In, Teresa Emery, Patrick Longhini, James Turtle					
			5e. TASK NUMBER		
			5f. WORK UNIT NUMBER		
7. PERFORMING ORGANIZATION NAMES AND ADDRESSES			8. PERFORMING ORGANIZATION REPORT NUMBER		
San Diego State University Foundation 5250 Campanile Dr. San Diego, CA 92182 -1931					
9. SPONSORING/MONITORING AGENCY NAME(S) AND ADDRESS(ES)			10. SPONSOR/MONITOR'S ACRONYM(S) ARO		
U.S. Army Research Office P.O. Box 12211 Research Triangle Park, NC 27709-2211			11. SPONSOR/MONITOR'S REPORT NUMBER(S)		
			60768-EG.2		
12. DISTRIBUTION AVAILABILITY STATEMENT					
Approved for public release; distribution is unlimited.					
13. SUPPLEMENTARY NOTES					
The views, opinions and/or findings contained in this report are those of the author(s) and should not be construed as an official Department of the Army position, policy or decision, unless so designated by other documentation.					
14. ABSTRACT					
Over the past few years it has been shown, through theory and experiments, that the AC current produced by spin torque nano-oscillators (STNO), coupled in an array, can lead to feedback between the STNOs causing them to synchronize and that, collectively, the microwave power output of the array is significantly larger than that of an individual valve. Other works have pointed, however, to the difficulty in achieving synchronization. The governing equations lead to a high-dimensional dynamical system with S_N symmetry, i.e., permutation symmetry of N					
15. SUBJECT TERMS					
Nano-oscillators, symmetry, bifurcations					
16. SECURITY CLASSIFICATION OF:			17. LIMITATION OF ABSTRACT	15. NUMBER OF PAGES	19a. NAME OF RESPONSIBLE PERSON
a. REPORT	b. ABSTRACT	c. THIS PAGE	UU		Antonio Palacios
UU	UU	UU			19b. TELEPHONE NUMBER
					619-594-6808

Report Title

Gluing bifurcations in coupled spin torque nano-oscillators

ABSTRACT

Over the past few years it has been shown, through theory and experiments, that the AC current produced by spin torque nano-oscillators (STNO), coupled in an array, can lead to feedback between the STNOs causing them to synchronize and that, collectively, the microwave power output of the array is significantly larger than that of an individual valve. Other works have pointed, however, to the difficulty in achieving synchronization. The governing equations lead to a high-dimensional dynamical system with S_N symmetry, i.e., permutation symmetry of N objects due to all-to-all coupling. Under the ARO grant, we have investigated a reduction of the modeling equations, via center Manifold and Normal form, and the possibility of applying the most recent results from related work on coupled Hamiltonian systems to explain the nature of the bifurcations.

REPORT DOCUMENTATION PAGE (SF298)
(Continuation Sheet)

Continuation for Block 13

ARO Report Number 60768.2-EG

Gluing bifurcations in coupled spin torque nano- ...

Block 13: Supplementary Note

© 2013 . Published in Journal of Applied Physics, Vol. Ed. 0 113, (11) (2013), ((11). DoD Components reserve a royalty-free, nonexclusive and irrevocable right to reproduce, publish, or otherwise use the work for Federal purposes, and to authorize others to do so (DODGARS §32.36). The views, opinions and/or findings contained in this report are those of the author(s) and should not be construed as an official Department of the Army position, policy or decision, unless so designated by other documentation.

Approved for public release; distribution is unlimited.

Gluing bifurcations in coupled spin torque nano-oscillators

James Turtle,¹ Katherine Beauvais,¹ Richard Shaffer,¹ Antonio Palacios,^{1,a)} Visarath In,² Teresa Emery,² and Patrick Longhini²

¹*Nonlinear Dynamical Systems Group, Department of Mathematics, San Diego State University, San Diego, California 92182, USA.*

²*Space and Naval Warfare Systems Center Pacific, Code 71730, 53560 Hull Street, San Diego, California 92152-5001, USA.*

(Received 10 October 2012; accepted 27 February 2013; published online 15 March 2013)

Over the past few years, it has been shown, through theory and experiments, that the AC current produced by spin torque nano-oscillators (STNO), coupled in an array, can lead to feedback between the STNOs causing them to synchronize and that, collectively, the microwave power output of the array is significantly larger than that of an individual valve. Other works have pointed, however, to the difficulty in achieving synchronization. In particular, Persson *et al.* [J. Appl. Phys. **101**, 09A503 (2007)] shows that the region of parameter space where the synchronization state exists for even a small array with two STNOs is rather small. In this work, we explore in more detail the nature of the bifurcations that lead into and out of the synchronization state for the two-array case. The bifurcation analysis shows bistability between in-phase and out-of-phase limit cycle oscillations. In fact, there are two distinct pairs of such cycles. But as the input current increases, the limit cycles may increase their amplitudes until they merge with one another in a gluing bifurcation. More importantly, we show that changing the direction of the applied magnetic field can, in principle, increase the region of synchronized oscillations. © 2013 American Institute of Physics. [<http://dx.doi.org/10.1063/1.4795266>]

I. INTRODUCTION

Spintronics—the emerging science that seeks to exploit the intrinsic spin of the electron—has stimulated scientists and engineers around the world to envision, design, and fabricate an entire new generation of smaller, faster, and more energy-efficient nano-electronic devices.¹ Spintronic devices work on the quantum mechanical effects of electrons having two-state spins, “up” or “down.” By running current through a ferromagnetic material, a spin-polarized current can be created and manipulated by magnetic fields. The most common application of this effect is the *spin nano-valve* device, which consists of at least two layers (about 100 nm in lateral size) of ferromagnetic materials separated by a nonmagnetic material layer, see Fig. 1. In one layer, the magnetization vectors are fixed while on the other hand they are free in order to exploit the giant magnetoresistive (GMR) effect. This effect is observed as a significant change in the electrical resistance of some materials depending on whether the magnetization of adjacent ferromagnetic layers is in antiparallel (high resistance) or in parallel (low resistance). One immediate application of the spin valve is as a sensor of weak fields. But a later discovery of the *spin-polarized phenomenon* may soon allow spin valves to be used also as miniaturized microwave signal generators.

Indeed, in 1996, Slonczewski³ and Berger² predicted the spin-polarized phenomenon in which a polarized current can exert a torque on the magnetization of a ferromagnetic layer. For large enough currents, this torque can lead to switching and/or precession of the magnetization, see Fig. 1. Then the

magnetic precession of the free layer can lead, through the GMR effect, to an oscillating dipolar field in the form of a microwave voltage signal and turn the valve into a *spin torque nano-oscillator* (STNO). This nano-oscillator is, in principle, tunable over a broad frequency band, about 40 GHz,⁴

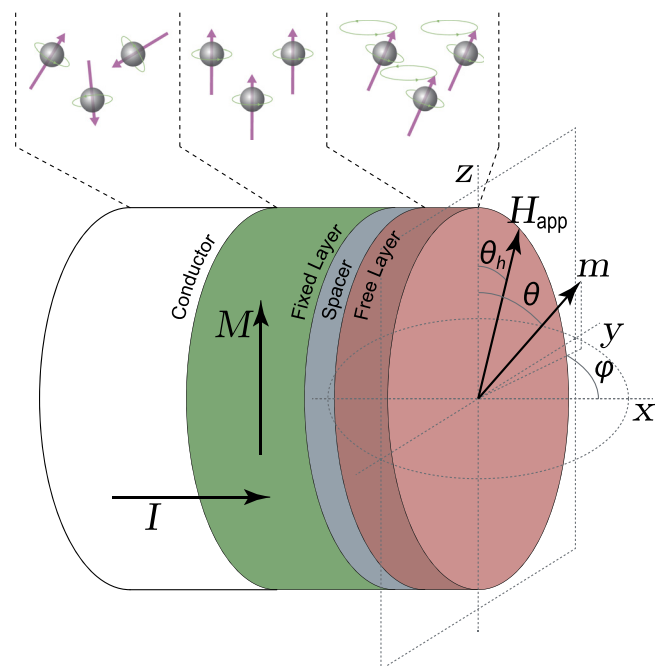


FIG. 1. Schematic representation of a spin torque nano-oscillator. This nano-oscillator consists of at least two layers (about 100 nm in lateral size) of ferromagnetic materials separated by a nonmagnetic material layer or spacer.

^{a)}Electronic mail: palacios@euler.sdsu.edu.

which renders it ideal for many applications, including: telecommunications, e.g., wireless systems; radar, e.g., air traffic control, weather forecasting, and navigation systems. But the microwave power emitted by a single valve is very small, about 1 nW,⁵ which is not adequate for on chip applications. A possible solution to this problem, which has been proposed by various groups,^{6–10} is to synchronize several STNOs so that a coherent signal with a common frequency and phase can be extracted from the ensemble to produce a more powerful (on the order of micro-watts) microwave signal. To date, there is no report, however, that even just five STNOs connected in series can be synchronized. Thus, an alternative solution to achieve practical power is to boost the power of a single STNO. Indeed, large power (over 1 μ W) in single STNOs has been recently demonstrated.¹¹ In this manuscript, we focus on the first alternative as we are motivated by all previous works that have tried to address the problem of synchronization.

As noted by the 2007 Nobel Laureate Professor Albert Fert: “the synchronization of STNOs raises complex problems that are new in spintronics and related to the general field of Dynamics of Nonlinear Systems.”⁶ Presumably, the problems that Professor Fert had envision include: understanding and classifying the various coherent states that an ensemble of STNOs can produce, finding conditions for the existence and stability of such coherent states, determining the effects of different couplings and connection topologies, establishing scaling laws of microwave power output for large 1D and 2D multi-layers, and conducting *transformative research* to translate theory into actual device realizations of STNOs. These problems, and many other related issues, remain open and are currently the subject of intense research efforts, analytically, computationally, and experimentally, across the world.

Thus, in 2005, Kaka and collaborators from the National Institute of Standards and Technology (NIST) reported in *Nature*,⁷ the first experiments that show that two spin torque nano-oscillators tend to phase lock when they are in close proximity of one another. The coupling in this case is “soft” as it depends on the magnetic fields produced by each nano-oscillator. Soon after, Grollier *et al.*⁶ investigated, computationally, the behavior of a 1D array of $N=10$ STNOs electrically coupled in series. Their study showed that the AC current produced by each individual oscillator can also lead to synchronization and that, collectively, the microwave power output of the array is significantly larger than that of an individual valve. In a follow-up study, Persson *et al.*⁸ mapped out numerically the region of synchronization of the 1D serially connected array considered by Grollier for the special case of $N=2$ STNOs. The critical observation, albeit disappointing, points out that synchronization is difficult to achieve because the region of parameter space where this regime exists is rather small. Subsequently, Li *et al.*¹² showed that this difficulty was due, mainly, to the coexistence of multiple stable attractors, which suggests that the synchronization regime is highly sensitive to initial conditions. On a more positive note, a joint effort by researchers from the Army Research Laboratory (ARL) and from NIST produced recently the first demonstration of the ability of a single

STNO to radiate energy through space.⁵ At about 250 pW and high frequency of 9 GHz, the generated signal carried lower power than expected from the previous theoretical studies⁷ but it was able to travel through air over a distance of 1 m.

In the present work, we provide a detailed description of the nature of the bifurcations that lead into and out of the synchronization regime in the 1D array of two serially connected STNOs considered by Persson *et al.*⁸ Although Persson’s work, and also our work, is focused on only two oscillators, we believe that a better understanding of the nature of the bifurcations in this small array can provide helpful insight to achieve synchronization in larger arrays. The bifurcation analysis shows bistability between in-phase and out-of-phase patterns of oscillations, which emerge via back-to-back Hopf bifurcations from a branch of nontrivial saddle-node equilibria. There are, in fact, two distinct pairs of such limit cycles. When the applied magnetic field occurs in a direction that leads to reflectional symmetry in the governing equations then it might be possible to manipulate only the input current to bring together the cycles until they merge with one another in a gluing bifurcation.¹³ But if the applied magnetic field breaks the symmetry of the equations then two parameters must be varied to glue together the cycles. This is the case because the gluing bifurcation is a global bifurcation that is facilitated by the presence of reflectional symmetry. That is, when reflectional symmetry is present in the system the cycles can be considered as mirror images of one another. Thus, generically, only one parameter needs to be varied to move the two cycles and the codimension of the bifurcation is one. In the absence of reflectional symmetry, each cycle can be moved independently of one another and thus the bifurcation becomes codimension two. While the symmetry of the system is important, from a mathematical standpoint, for the creation of the gluing bifurcation the critical observation that we wish to emphasize from a physics standpoint is that the bistability of the out-of-phase oscillations is what seems to make the synchronization state very difficult to achieve. As the basins of attraction of these two solutions compete for stability, it appears that the volume of phase space that the basin of attraction of the out-of-phase solution occupies is much larger than that of the synchronization regime. The good news is, however, that a change in the direction of the applied field can significantly enlarge the basin of attraction of the synchronization state and reverse the preferred state towards synchronization. This type of enhanced synchronization offers an alternative to the use of delays as it was originally proposed by Persson *et al.*⁸ Another bit of good news is that the synchronization regime appears to be significantly robust to fluctuations of parameters and, in turn, to variations in the frequency of oscillation of each individual spin valve. In particular, when the spin valves are non-identical, differences in the anisotropy and demagnetization fields and gyromagnetic ratio can lead to dispersion among the free-evolving frequency of each individual spin valve. However, careful tuning of the DC current and of the resistors in the circuit can lead the array to overcome the frequency mismatch and for the system dynamics to evolve towards the synchronization attractor. This result is

expected because numerical computations show that all Lyapunov exponents transverse to the synchronization manifold are negative; so that small perturbations or fluctuations in system parameters can be absorbed by the array while the solution trajectories asymptotically converge to the synchronization state. From the standpoint of the bifurcation analysis, we also wish to emphasize that differences in parameter values tend to shift the onset of oscillations shown in the computational bifurcation diagrams while the overall structure of the diagrams is preserved. We do not attempt in this work to quantify the frequency mismatch nor the shift in the location of the Hopf bifurcations that lead to limit cycle oscillations. Those tasks, and a more comprehensive analysis of the effects of the nonhomogeneity of parameter values and an investigation of stochastic effects, such as noise in the system, are part of ongoing work. We expect to report those results in a follow-up manuscript.

II. MODELING

A. Single STNO dynamics

An originally unpolarized electric current I , in units of Amp, is applied to a fixed magnetic layer whose magnetization is represented by \hat{M} . As the electrons pass through the layer, their spins move (and flip if necessary) to align their orientations to that of the fixed layer, thus, creating a *spin-polarized* current, see Fig. 1 for a schematic diagram.

The electrical potential that exists across the nonmagnetic layer (labeled spacer) allows the spin-polarized current to preserve its polarization. So when the spin-polarized current enters the free magnetic layer, it exerts a torque on its magnetization \hat{m} . According to Newton's third law, the amount of torque is directly proportional (and of opposite sign) to the difference in the magnetization of the spins in the polarized current and those of the free layer. We will assume the layers to be uniform so that the spin precession is proportional to $-\hat{m} \times \vec{H}_{\text{eff}}$, where \vec{H}_{eff} is the effective magnetic field, which consists of the exchange field, $\vec{H}_{\text{exchange}}$, among magnetic moments, a surface anisotropy field, $\vec{H}_{\text{anisotropy}}$, which defines a preferred direction of magnetization, a demagnetization field $\vec{H}_{\text{demagnetization}}$, and the applied magnetic field \vec{H}_{applied} . Collectively, the effective field becomes

$$\vec{H}_{\text{eff}} = \vec{H}_{\text{exchange}} + \vec{H}_{\text{anisotropy}} + \vec{H}_{\text{demagnetization}} + \vec{H}_{\text{applied}}.$$

Also it can be shown that the spin-transfer torque is proportional to $\hat{m} \times (\hat{m} \times \hat{M})$. Energy dissipation effects such as those due to spin scattering lead to a damping term proportional to $\hat{m} \times \frac{d\hat{m}}{dt}$. Together, these quantities govern the dynamics of the free magnetization layer through the Landau-Lifshitz-Gilbert-Slonczewski (LLGS)^{2,14-17} equation:

$$\frac{d\hat{m}}{dt} = \underbrace{-\gamma \hat{m} \times \vec{H}_{\text{eff}}}_{\text{precession}} + \underbrace{\lambda \hat{m} \times \frac{d\hat{m}}{dt}}_{\text{damping}} + \underbrace{-\gamma a g(P, \hat{m} \cdot \hat{M}) \hat{m} \times (\hat{m} \times \hat{M})}_{\text{spin transfer torque}}, \quad (1)$$

where γ is the gyromagnetic ratio, in units of $\frac{1}{\text{Oe ns}}$, where ns represents nanoseconds, while λ serves as the magnitude of the damping term, in dimensionless units. In the spin torque term, a has a unit of Oe and is proportional to the electrical current density^{14,18,19} which can be written as $a = \frac{\hbar I_j}{2S_0 V e}$, where S_0 is the constant magnitude of the average magnetization vector $S(t)$, in units of Oe, so that $\hat{m} = \vec{S}/S_0$ is the dimensionless unit vector in the direction of S , g is a function of the polarization factor P , which will be assumed to be exactly one in dimensionless units. $\hbar = 6.582 \times 10^{-16}$ is Planck's constant in units of eV s, $V = 3.0732$ is volume in units of cm^3 , $e = 1.602 \times 10^{-19}$ is the elementary charge in units of Coulombs.

B. Series array of STNOs

We now consider a 1D array of STNOs connected in series, as is shown in Fig. 2, and derive the governing equations for the general case of N STNOs though the remaining work is focused on the particular case of $N=2$ studied by Persson *et al.*⁸

Following the work of Grollier *et al.*,⁶ we assume the standard equation for the resistance (in units of Ω) of the i th oscillator to be $R_i(t) = R_{0i} - \Delta R_i \cos \theta_i(t)$, where $\theta_i(t)$ is the angle between the magnetization of the fixed and free ferromagnetic layers, R_{0i} is the mean while ΔR_i is half the difference between the resistances in the parallel, R_{Pi} , and the anti-parallel, R_{APi} , magnetization states, respectively. That is, $R_{0i} = (R_{APi} + R_{Pi})/2$ and $\Delta R_i = (R_{APi} - R_{Pi})/2$. The input I_0 is a known DC current. To determine the instantaneous current through the j th STNO element, we combine Kirchoff's Current Law and Ohm's Law to produce a simple current divider equation:

$$I_j = \frac{R_C}{\sum_{i=1}^N R_i + R_C} I_0. \quad (2)$$

Because the right-hand side of Eq. (2) is independent of j , the current must be the same in all oscillators. Removing the j index and substituting R_i into Eq. (2) produces, after some manipulation, the following equation for the current:

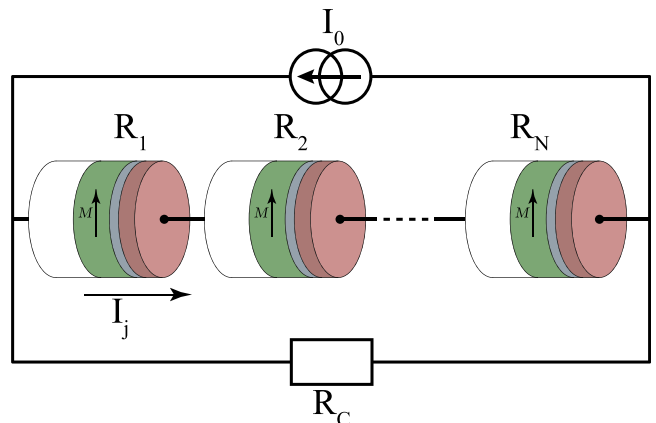


FIG. 2. Circuit array of spin torque nano-oscillators connected in series.

$$I(t) = \frac{\frac{R_C}{R_C + \sum_{i=1}^N R_{0i}}}{1 - \frac{\sum_{i=1}^N \Delta R_i \cos \theta_i(t)}{R_C + \sum_{i=1}^N R_{0i}}} I_0. \quad (3)$$

Notice that the numerator is time invariant. In fact, this numerator is a good approximation for the DC current in the oscillator circuit branch. Expanding Eq. (3) in a first order Taylor approximation, we can rewrite $I(t)$ in the simplified form:

$$I(t) = I_{DC} \left(1 + \sum_{i=1}^N \beta_{\Delta R_i} \cos \theta_i(t) \right), \quad (4)$$

where

$$I_{DC} = \frac{R_C}{R_C + \sum_{i=1}^N R_{0i}} I_0 \quad \text{and} \quad \beta_{\Delta R_i} = \frac{\Delta R_i}{R_C + \sum_{i=1}^N R_{0i}}.$$

We note that the current I appears in the spin torque term of the LLGS Eq. (1) through the parameter a . Thus, assuming a polarization factor $g = 1$, we arrive at the following model for the array of N STNOs electrically coupled in series

$$\begin{aligned} \frac{d\hat{m}_j}{dt} = & -\gamma \hat{m}_j \times \vec{H}_{eff} + \lambda \hat{m}_j \times \frac{d\hat{m}_j}{dt} \\ & - \gamma \frac{\hbar}{2S_0 V e} I_{DC} \left(1 + \sum_{i=1}^N \beta_{\Delta R_i} \cos \theta_i(t) \right) \hat{m}_j \times (\hat{m}_j \times \hat{M}). \end{aligned} \quad (5)$$

It is observed from Eq. (5) that the series configuration results in an all-to-all coupling scheme where each individual STNO is influenced by the angles between the free and fixed layers of every other STNO. Thus, the symmetries of

the series array of N STNOs are described by the group S_N , which is the group of all permutations of N objects. While these equations are valid for up to $j = 1 \dots N$ oscillators, our aim in this work is to focus on the case $N = 2$ considered by Persson *et al.*⁸ But first we conduct computer simulations of the governing equations (5) in order to get insight into the type of transitions that lead to the synchronization state. We employ the relations introduced by Murugesu and Lakshmanan^{18,19} for the following terms: $\vec{H}_{anisotropy} = \kappa(\hat{m} \cdot \hat{e}_{||})\hat{e}_{||}$, where $\kappa = 45$ Oe, $e_{||} = [\sin\theta_{||}\cos\phi_{||}, \sin\theta_{||}\sin\phi_{||}, \cos\theta_{||}]^T$ is dimensionless, $\vec{H}_{demagnetization} = -4\pi S_0(N_1 m_1 \hat{x} + N_2 m_2 \hat{y} + N_3 m_3 \hat{z})$, where N_i , $i = 1, 2, 3$ are dimensionless constants with $N_1 + N_2 + N_3 = 1$, and $\{\hat{x}, \hat{y}, \hat{z}\}$ are the orthonormal unit vectors. However, we deviate slightly in considering the applied magnetic field to lie on the yz -plane instead of the z -axis, so that $\vec{H}_{applied} = h_a[0, \sin\theta_h, \cos\theta_h]^T$, where h_a is in units of Oe. In what follows we assume the direction of demagnetization to be along the \hat{x} -axis so that $N = [1, 0, 0]^T$, thus, creating a yz -plane. We also assume $\theta_{||} = 0$ so that $e_{||} = [0, 0, 1]$, which produces an easy axis in the z -direction. Finally, we assume the direction of polarization of the spin-polarized current to remain constant along the z -direction $\hat{M} = \hat{z}$.

In the computational work of Persson *et al.*,⁸ it was reported that the magnetization states $m_j(t)$ relax to stable equilibrium states for small and for very large positive values of the input DC current, I_{DC} . It was also reported that non-synchronized oscillations occur for most intermediate values of I_{DC} while synchronized oscillations are rare—as they occur on very small regions neighboring the equilibrium states. Something very similar occurs in our simulations, see Figure 3, except that now the large values of current where equilibrium states appear are negative. This inversion of sign is due to the fact that in our formulation of the LLGS Eq. (1) we have employed the notation introduced by Lakshmanan,¹⁵ which contains a negative sign in front of the gyromagnetic ratio γ as oppose to the positive sign used by Persson *et al.* Up to a conjugacy in sign, these two formulations are equivalent. So we can proceed with the exploration of the dynamics. As reported by Persson *et al.*, our simulations show that for

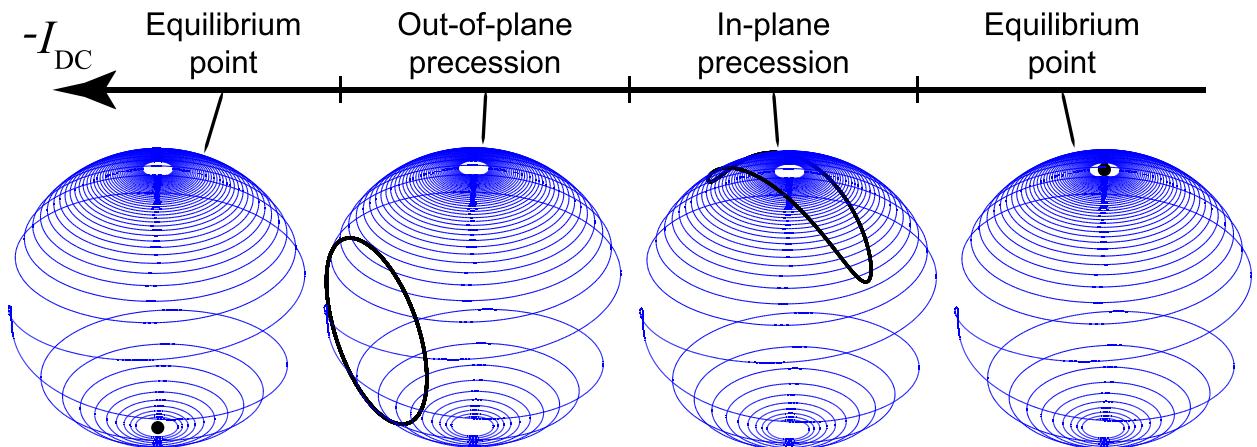


FIG. 3. Collective behavior of two STNOs coupled in a series array through an external electrical current I_{DC} . Parameters are: $\gamma = 0.0176 \frac{1}{\text{Oe ns}}$, $\lambda = 0.008$, $\theta_{||} = 0$ rad, $\theta_h = 0$ rad, $h_a = 300$ Oe, $\kappa = 45$ Oe, $S_0 = 8400/(4\pi)$ Oe, $\hat{N} = [1, 0, 0]^T$, $R_{0i} = 0.1 \Omega$, $R_C = 50 \Omega$, and $\Delta R_i = 0.03 \Omega$.

intermediate values of I_{DC} the dynamics is attracted to stable limit cycle oscillations. There are, indeed, two types of limit cycles. One of them corresponds to the out-of-phase oscillations, OP, where the two magnetization states oscillate with the same waveform and amplitude but out of phase by half a period. The other cycle corresponds to the in-phase oscillations, IP, leading to a complete synchronization state. Next we study in more detail the nature of the bifurcations that lead into/out-of the synchronization state. We would like to emphasize that such bifurcation study was not discussed in Persson *et al.*⁸ but it can be an important tool to help us look for clues to increase the region of stability of the synchronized pattern of collective behavior with the ultimate goal of achieving higher power output through an array of spin valves.

III. COMPUTATIONAL BIFURCATION ANALYSIS

In order to understand the nature of the bifurcations that lead into and out of the synchronization state, we perform next a computational bifurcation analysis, with the aid of the continuation software package AUTO,²⁰ of the governing equations. For convenience, we convert to complex stereographic coordinates^{18,19} through the following change of variables:

$$z_j = \frac{m_{j1} + im_{j2}}{1 + m_{j3}}. \quad (6)$$

Direct and tedious calculations using Eq. (6) lead to the following set of differential equations in stereographic coordinates:

$$\begin{aligned} (1 - i\lambda) \frac{dz_j}{dt} = & -\gamma a z_j + i\gamma h_{a3} z_j + \frac{\gamma h_{a2}}{2} (1 + z_j^2) \\ & + im_{j1} \kappa \gamma \left[\cos\theta_{||} z_j - \frac{1}{2} \sin\theta_{||} (e^{i\phi_{||}} - z_j^2 e^{-i\phi_{||}}) \right] \\ & - \frac{i\gamma 4\pi S_o}{(1 + |z_j|^2)} \left[N_3 (1 - |z_j|^2) z_j \right. \\ & - \frac{N_1}{2} (1 - z_j^2 - |z_j|^2) z_j - \frac{N_2}{2} (1 + z_j^2 - |z_j|^2) z_j \\ & \left. - \frac{(N_1 - N_2)}{2} \bar{z}_j \right]. \end{aligned} \quad (7)$$

As a first case, we set $\theta_h = 0$ so that the applied magnetic field \vec{H}_{applied} lies exactly along the z -axis as it was originally considered by Persson *et al.*⁸ We then use Eq. (7) to generate the one-parameter bifurcation diagram in Fig. 4, which illustrates how the magnetization state changes as a function of input current. As expected, for positive, small and large values of the input current, the magnetization state relaxes to the stable trivial or zero equilibrium state, which is indicated as a solid (red) line. For large negative values of the input current, in particular, two branches of nontrivial stable equilibrium points emerge via the saddle node bifurcations, labeled SN_1 and SN_2 . Along these branches, the spin valves cannot oscillate, as they remain in a steady state. Many other equilibrium points also exist over a wide range of values of I_{DC} but they are mostly unstable (dashed line). As the input current increases from the saddle-node

bifurcation points SN_1 , the nontrivial equilibrium point remains almost constant until it loses stability and two branches of periodic solutions then emerge via back-to-back Hopf bifurcations, labeled HB_4 and HB_5 . One branch (blue) corresponds to the out-of-phase pattern, OP, and the other one (green) corresponds to the complete synchronization state, IP. It is not surprise that these are the only oscillations that appear for they are the most common patterns of collective behavior observed in a system of two identical oscillators coupled symmetrically, as it the case of our STNO array. Furthermore, it can be shown that the oscillations emerge through symmetry-breaking bifurcations in which the synchronous state preserves the S_2 symmetry of the array while the out-of-phase pattern breaks it. Now, since the magnetic field was applied directly along the z -axis, the governing equations exhibit also a reflectional Z_2 symmetry for the internal dynamics of each individual spin valve, which manifests as a mirror-image symmetry across the $X_1 = 0$ axis in the bifurcation diagram. This symmetry leads to a second pair of limit cycle oscillations that emerge from the back-to-back Hopf points HB_2 and HB_3 with the same characteristics as those of HB_4 and HB_5 . Now as the coupling DC current I_{DC} increases the amplitude of the limit cycles in each branch increases gradually until the cycles merge with one another in a gluing bifurcation near $I_{DC} = 0$. The onset of the gluing bifurcation occurs just before the Hopf bifurcation HB_1 , which appears off of the trivial equilibrium.

Additionally, we wish to emphasize that when the spin valves are non-identical, fluctuations in system parameters, such as anisotropy and demagnetization fields and gyromagnetic ratio, can shift the onset of the Hopf bifurcation points that lead to limit cycle oscillations. However, the overall structure of the bifurcation diagrams remains the same provided that the fluctuations are not extremely large. In a follow-up manuscript, we plan to explore the effects of the nonhomogeneity of parameter values as well as the effects of noise on the bifurcation structure.

Up to now, we have described somehow mathematically complex behaviors associated with the bifurcation diagrams, as illustrated in Fig. 4, where IP and OP oscillations overlap across a wide range of I_{DC} values. From an experimental physics standpoint, our main interest is to better understand the conditions for the existence and stability properties of the synchronization behavior, as it can provide benefits in operating an array of STNOs to increase the overall radiative power. The regions of existence are outlined through the bifurcation diagrams while the stability properties can be studied through many different approaches. One such approach is to compute the transverse Lyapunov exponents (TLE) of the synchronization manifold^{21,22} of the coupled system. To do this, we start by re-scaling time so that $\tau = \frac{\gamma}{1+\lambda^2} t$ and replace the complex stereographic coordinates $z_j, j = 1, 2$, with real coordinates (x_j, y_j) , where $z_j = x_j + y_j i$, so that the governing Eq. (7) becomes

$$\begin{aligned} \dot{x}_j &= f(x_j, y_j) + h_1(x_1, y_1, x_2, y_2), \\ \dot{y}_j &= g(x_j, y_j) + h_2(x_1, y_1, x_2, y_2), \end{aligned} \quad (8)$$

where

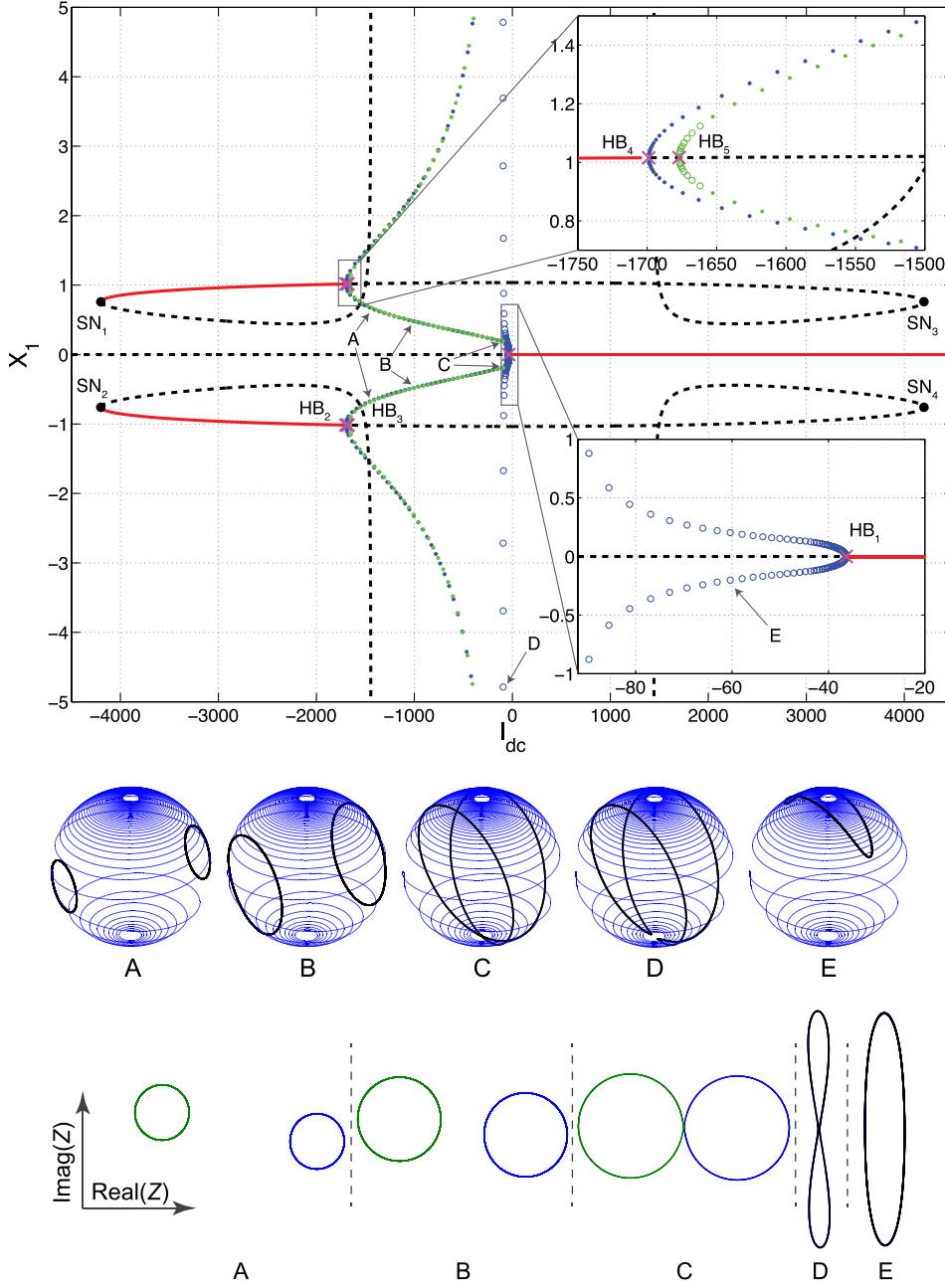


FIG. 4. (Top) One parameter bifurcation diagram of changes in magnetization in a 1D array of $N = 2$ STNOs connected in series. Blue circles indicate out-of-phase oscillations while green circles indicate synchronized limit cycle oscillations. Filled-in (empty) circles indicate stable (unstable) oscillations. (Middle) Visualization of the dynamics on the unit sphere and (bottom) on the stereographic plane. Parameters are: $\gamma = 0.0176 \frac{1}{\text{Oe ns}}$, $\lambda = 0.008$, $\theta_{||} = 0$ rad, $\theta_h = 0$ rad, $h_a = 300$ Oe, $\kappa = 45$ Oe, $S_0 = 8400/(4\pi)$ Oe, $\hat{N} = [1, 0, 0]^T$, $R_{0i} = 0.1 \Omega$, $R_c = 50 \Omega$, and $\Delta R_i = 0.03 \Omega$.

$$\begin{aligned}
 f(x_j, y_j) &= -\lambda h_{a3} x_j - h_{a3} y_j - \kappa \left(\frac{1 - r_j^2}{1 + r_j^2} \right) (\lambda x_j + y_j) \\
 &\quad + \frac{h_{a2}}{2} (1 + x_j^2 - 2\lambda x_j y_j - y_j^2) \\
 &\quad + \frac{4\pi S_0}{1 + r_j^2} (\lambda x_j^3 + 2x_j^2 y_j - \lambda x_j y_j^2 - \lambda x_j), \\
 g(x_j, y_j) &= h_{a3} x_j - \lambda h_{a3} y_j + \kappa \left(\frac{1 - r_j^2}{1 + r_j^2} \right) (x_j - \lambda y_j) \\
 &\quad + \frac{h_{a2}}{2} (\lambda + \lambda x_j^2 + 2\lambda x_j y_j - \lambda y_j^2) \\
 &\quad + \frac{4\pi S_0}{1 + r_j^2} (-x_j^3 + 2\lambda x_j^2 y_j + x_j y_j^2 + x_j),
 \end{aligned}$$

represent the internal dynamics of the x_j and y_j components of the j th nano-oscillator, respectively, and $r_j^2 = x_j^2 + y_j^2$. The

terms h_j are the (all-to-all) coupling functions that connect the two nano-oscillators together, they are given by

$$\begin{aligned}
 h_1(x_j, y_j) &= -ax_j + ay_j, \\
 h_2(x_j, y_j) &= -a\lambda x_j - ay_j.
 \end{aligned}$$

The coupling strength is set by the parameter a . If we assume that all the oscillators have the same resistance $R_{0i} = R_0$ and magnetoresistance $\Delta R_i = \Delta R$ then the coupling strength for $N = 2$ can be written as

$$a = \frac{\hbar}{2S_0 V e} I_{DC} \left(1 + \frac{A_{GMR}}{N} \sum_{j=1}^N \frac{1 - r_j^2}{1 + r_j^2} \right), \quad A_{GMR} = \frac{\Delta R}{\frac{R_c}{N} + R_0}.$$

Let $u_j = (x_j, y_j)$, $j = 1, 2$. We now transform Eq. (8) to the transversal coordinates $x_{\perp} = u_1 - u_2$ and consider only small perturbations to the synchronization manifold, i.e.,

$u_1 \approx u_2$. Then the dynamics along the transverse direction to the synchronization manifold becomes

$$\begin{aligned}\dot{x}_{\perp 1} &= f(x_1, y_2) - f(x_2, y_2) - ax_{\perp 1} + a\lambda x_{\perp 2}, \\ \dot{x}_{\perp 2} &= g(x_1, y_2) - g(x_2, y_2) - a\lambda x_{\perp 1} - ax_{\perp 2}.\end{aligned}\quad (9)$$

We can now proceed in two ways. Expand $f(x_2, y_2)$ in a Taylor's series expansion about (x_1, y_1) or expand $f(x_1, y_1)$ about the second coordinate. We choose the former approach for both f and g , and also for the terms in a . Neglecting higher order terms of x_{\perp} , we obtain, in matrix form, the linearization of Eq. (8) transverse to the synchronization manifold

$$\dot{x}_{\perp} = (J + K)x_{\perp}, \quad (10)$$

where J is the Jacobian matrix of the vector field $F = (f(x, y), g(x, y))$ evaluated at the synchronization manifold, i.e., $J = dF_{(x_s, y_s)}$, where $x_s = x_1 = \dots, x_N, y_s = y_1 = \dots, y_N$, and K is the matrix that results from the linearization of the coupling terms

$$K = \frac{\hbar}{2S_0Ve} I_{DC} \times \begin{bmatrix} -1 - A_{GMR} \left(\frac{1-r^2}{1+r^2} \right) & \lambda + \lambda A_{GMR} \left(\frac{1-r^2}{1+r^2} \right) \\ -\lambda - A_{GMR} \left(\frac{1-r^2}{1+r^2} \right) & -1 - A_{GMR} \left(\frac{1-r^2}{1+r^2} \right) \end{bmatrix}.$$

The synchronization state $u_1 = u_2$ is said to be asymptotically stable if $x_{\perp} \rightarrow 0$ as $t \rightarrow \infty$ or if the transverse Lyapunov exponents, which are the Lyapunov exponents associated with the linearized equations (10), are all negative. Numerical computations, see Fig. 5, reveal that the sum of TLEs is always negative except for the interval $I_{DC} \in [-1700, -1660]$, which is enhanced in the inset. Recall from the one-parameter bifurcation diagram of Fig. 4 that the subinterval $I_{DC} \in [-1700, -1675]$ is the region between the Hopf points HB_4 and HB_5 where only the out-of-phase solution exists, so the calculation of TLEs picks up the instability of the unstable non-trivial steady state and that

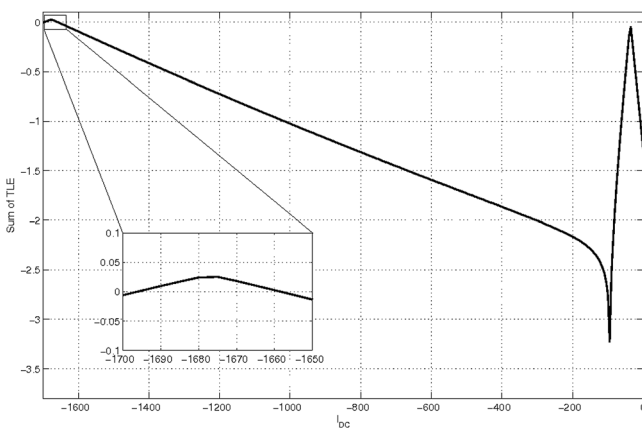


FIG. 5. Transverse Lyapunov exponents computed as a function of input current for an array of $N=2$ STNOs connected in series with applied field along the z -direction, i.e., $\theta_h = 0$ rad. All other parameters are the same as in Fig. 4.

explains why the sum of TLEs is positive. As I_{DC} reaches the right-end of that subinterval, the synchronized solution emerges via a subcritical Hopf bifurcation at HB_5 , so the sum of TLEs is still negative. However, as I_{DC} increases further within the subinterval $I_{DC} \in [-1675, -1660]$, the synchronized pattern becomes less unstable and the sum of TLEs decreases until it eventually crosses zero near $I_{DC} = -1660$, at which point the synchronized state becomes stable. From then on, the sum of TLEs decreases monotonically while the synchronized pattern increases stability until the gluing bifurcation point is reached near $I_{DC} \approx -100$. Past this point, the sum of TLEs increases until I_{DC} reaches the Hopf point HB_1 . To the right of HB_1 the trivial equilibrium is stable and so the sum of TLEs is negative. Similarly, in the region where the sum of TLEs is negative, all individual TLEs are also negative; though, they are not shown for brevity. Consequently, in that region there is a contraction of the phase space volume of the dynamics that is transversal to the synchronization manifold.²³ Negative TLEs also account for the robustness exhibited by the synchronization state to fluctuations in parameters. Indeed, we have verified through computer simulations that when the spin valves are non-identical, changes in the anisotropy and demagnetization fields and gyromagnetic ratio can lead to dispersion among the free-evolving frequency of each individual spin valve. Small frequency dispersions can still lead the system dynamics towards the synchronization attractor by careful tuning of the DC current and/or the resistors in the circuit which in turn control the parameter A_{GMR} . We do not attempt, however, to measure the largest dispersion that can be overcome by the system. That task is part of ongoing work.

Now, since the nano-oscillators are mutually coupled in an all-to-all fashion, the synchronized state may not necessarily be globally asymptotically stable and may still depend on initial conditions. Indeed, we already know from the bifurcation diagram that the out-of-phase solution coexists and is stable within the same parameter region of the synchronization state. Each one of these solutions has its own basin of attraction. We do not attempt in this work to visualize those basins of attraction. However, we try to get a sense of their size by measuring the coherence parameter, also known as the Kuramoto^{24,25} order parameter

$$r = \frac{1}{N} \left| \sum_{k=1}^N e^{i\phi_k} \right|, \quad 0 \leq r \leq 1.$$

In Fig. 6, we compute the Kuramoto^{24,25} order parameter r when $\theta_h = 0$ over a region where one of the pairs of limit cycles coexist as a function of DC current. This parameter serves as a measure of coherence of the phase dynamics of an ensemble of oscillators. Indeed, direct calculations show that when $r=0$ the phase dynamics is asynchronous while $r=1$ corresponds to full or complete synchronization. Intermediate values of r can be associated with more complicated states where the oscillators organize themselves into clusters of in-phase, traveling waves, and other related patterns. Thus, the calculation of the coherence parameter suggests that when $\theta_h = 0$ the coupled system is highly sensitive to changes in input current. Sometimes the phase dynamics of the two nano-

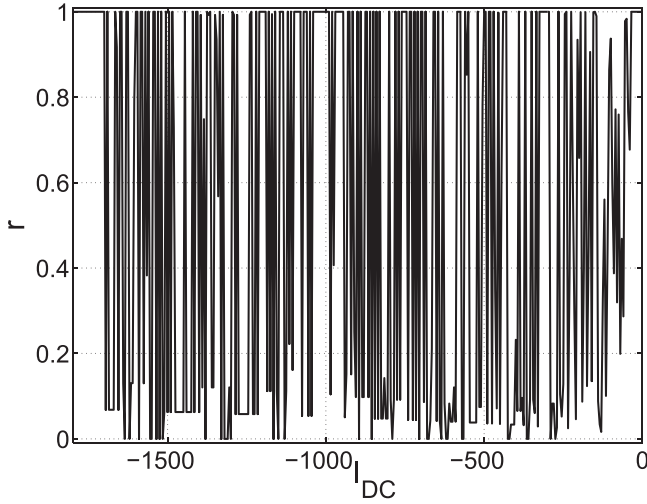


FIG. 6. Coherence parameter r computed as a function of input current for an array of $N=2$ STNOs connected in series with applied field along the z -direction, i.e., $\theta_h = 0$ rad. $r=1$ is associated with full synchronization while $r=0$ is indicative of asynchronous behavior. Parameters are the same as in Fig. 4.

oscillators synchronize but then a slight change in the input current can easily push the system in and out of the synchronization state. The transitions from one pattern of oscillation to another do not occur, in general, instantaneously so r can fluctuate slightly between zero and one. Presumably we could correct those fluctuations by integrating for longer periods of time. However, we would like to point out that we are already integrating the equations for a very long time interval, so further increases can yield minor changes in r . More importantly, the lack of large open intervals where r could remain close to one, see Fig. 6, suggest that the basin of attraction of the synchronized oscillations occupies a relatively small volume of phase space. This, again, confirms the observation by Persson *et al.*⁸ that “nonsynchronized precession largely dominates the phase diagram.” Similar results are obtained for the other pair of limit cycles.

Figure 7 shows the two-parameter continuation of the Hopf bifurcation points $HB_1 - HB_5$ and saddle-node points, in parameter space κ vs I_{DC} . Recall that κ is a coefficient associated with the anisotropy field. For small values of κ , the Hopf points HB_2, \dots, HB_5 are significantly separated from the saddle-node points SN_1 and SN_2 , as is the case in the one-parameter bifurcation diagram of Fig. 4. As κ increases, however, the locus of the back-to-back Hopf points move closer to that of the saddle-nodes, which remain almost constant. At the same time, the region of stable synchronized limit cycle solutions, shaded gray, starts to shrink. For significantly larger values of κ , the locus of the Hopf point has merged with the locus of the saddle-node points and the region of stable limit cycle in-phase oscillations has all but disappeared. For completeness purposes, the bifurcation diagram is carried out over negative values of κ . Observe that the loci of the Hopf points HB_2, \dots, HB_4 meet the almost circular curve that defines the loci of pitchfork bifurcations of nontrivial equilibrium points. These equilibrium states are the continuation of the saddle-node points for small negative values of κ , so they do not show up in Fig. 4.

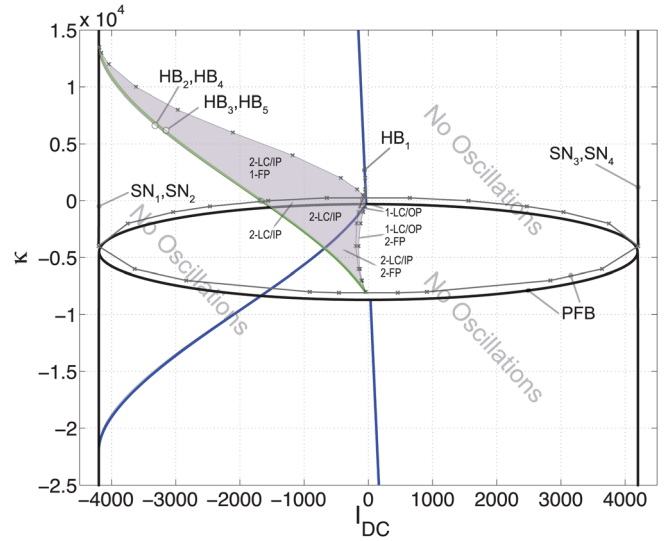


FIG. 7. Two parameter bifurcation diagram depicts the boundary curves, as functions of input current and anisotropy coefficient, which separate equilibrium states from limit cycle oscillations in a 1D array of $N=2$ STNOs connected in series. IP/OP indicate in-plane and out-of-plane oscillations, respectively. Parameters are the same as in Fig. 4 but we emphasize $\theta_h = 0$ rad.

Applying the magnetic field with a small angle along the y -direction, e.g., $\theta_h = \pi/4$, breaks the Z_2 -symmetry of the governing equations but the one- and two-parameter bifurcation diagrams exhibit similar characteristics to the perfectly symmetric case, i.e., $\theta_h = 0$, as is shown in Fig. 8(left). That is, there are two pairs of branches of periodic oscillations, each pair contains a branch of synchronized limit cycle oscillations and a branch of out-of-phase oscillations. The two pairs might merge together again in a gluing bifurcation. However, in the absence of the Z_2 -symmetry, it may be necessary to vary two parameters simultaneously for the gluing of the limit cycles to occur. This result shows that the reflectional Z_2 symmetry is important to generate the gluing bifurcation via a codimension one bifurcation; otherwise the codimension is two. As we discussed earlier, the two patterns of oscillations emerge again via symmetry-breaking bifurcations of the network, and in which the synchronized state preserves the S_2 symmetry of the array while the out-of-phase state breaks it. Now a critical observation is that if the angle of the applied field is further increased, e.g., $\theta_h = 3\pi/4$, then it is possible for the IP and OP branches of oscillations to switch position, as is shown in the one-parameter bifurcation of Fig. 8(right). This is a critical observation because the switch leads to an interval of the DC current where only the synchronized state is stable while the OP solution is unstable. Thus, in principle, on this interval it should be easier to achieve synchronization. Furthermore, we can see in Fig. 9(left) that, when $\theta_h = \pi/4$, small open intervals where $r \approx 1$ start to appear throughout the region where the two limit cycles, IP and OP, coexist. This suggests that a slight change in the direction of the applied field can facilitate the existence of the synchronization state. Indeed, increasing θ_h further to $3\pi/4$ shows, see Fig. 9(right), a very large open interval of DC current where the coherence parameter r is, approximately, equal to one. Thus, changing the direction of the applied field appears to have the net effect of changing the

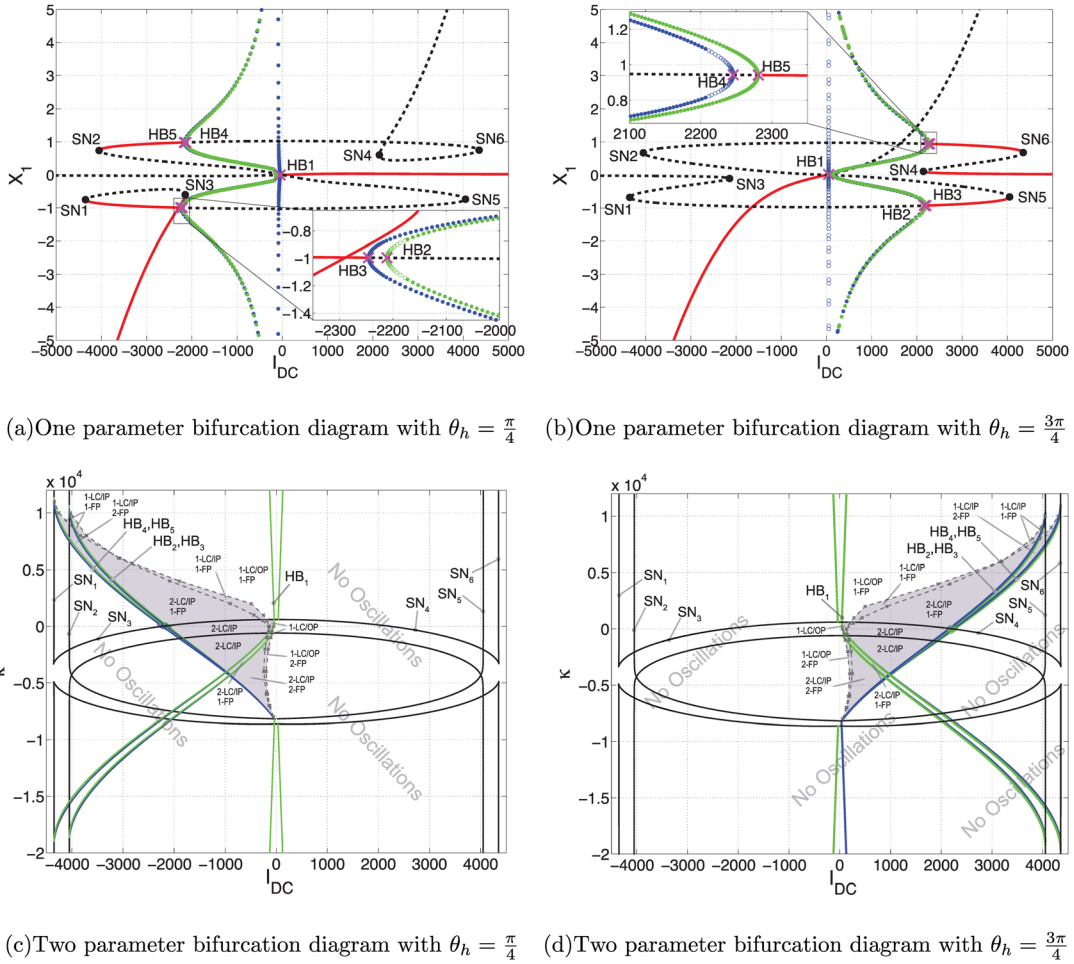


FIG. 8. One- and two-parameter bifurcation diagrams indicating regions of existence and stability of equilibrium states and limit cycle oscillations for a 1D array of $N = 2$ STNOs connected in series, with $\theta_h = \pi/4$ rad and $\theta_h = 3\pi/4$ rad. All other parameters are the same as in Fig. 4.

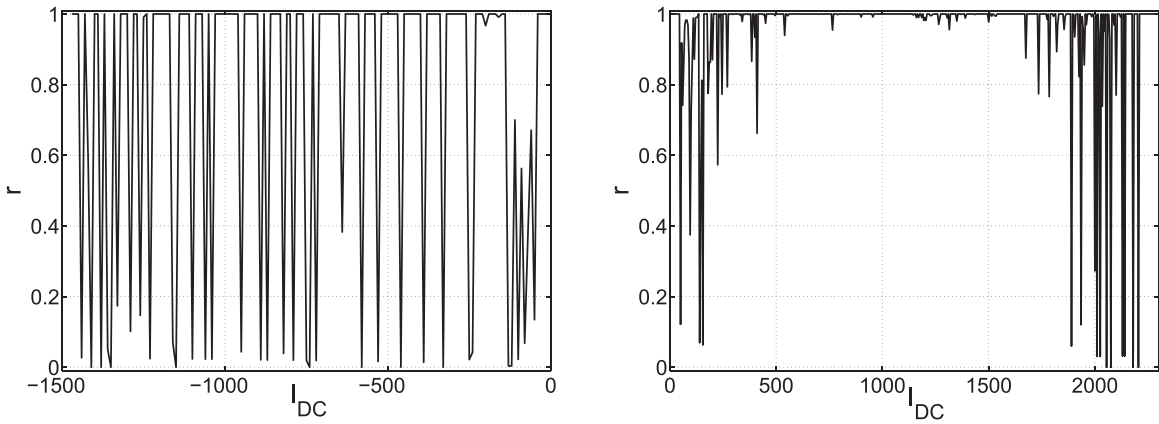


FIG. 9. Coherence parameter r computed as a function of input current for an array of $N = 2$ STNOs connected in series with applied field defined by (left) $\theta_h = \pi/4$ rad and (right) $\theta_h = 3\pi/4$ rad. All other parameters are the same as in Fig. 4.

basin of attractions so that the one associated with the IP solution now dominates a larger volume of phase space. This change is already a significant improvement in achieving synchronization especially when we compare Figs. 6 and 9.

IV. CONCLUSION

In this work, we have studied the collective behavior of an array of spin torque nano-oscillators connected in series.

The derivation of the governing equations for the array leads to an all-to-all S_N symmetric coupled system of ordinary differential equations, in which each individual nano-oscillator is modeled through the Landau-Lifshitz-Gilbert-Slonczewski equation. A computational bifurcation analysis, focused on two nano-oscillators, shows transitions between equilibrium states and limit cycle oscillations in a manner that is consistent with related studies conducted by other researchers. In particular, the bifurcation diagrams reveal two patterns of

collective behavior: an in-phase pattern, in which all oscillators are fully synchronized with one another, and an out-of-phase pattern. These two patterns are generic, i.e., most common, solutions in arrays of two identical oscillators coupled symmetrically. Furthermore, the presence of reflectional symmetry in the internal dynamics of each nano-oscillator leads naturally to gluing bifurcations of these two cycles. However, of greater interest from a physics standpoint is the region of existence and stability properties of the in-phase pattern because synchronized oscillations can, in principle, yield higher microwave power output. Previous works have shown that such pattern is rather difficult to realize. The work conducted in this manuscript provides answers to circumvent this difficulty. More specifically, the bifurcation analysis and measures of coherence presented in this manuscript reveal that a change in the direction of the applied field can significantly enhance the basin of attraction of the synchronous state without the need of adding delay into the model equations. Work in progress includes visualization of the basins of attraction and a similar analysis of the collective behavior of larger arrays, which we can expect to show more complicated patterns of oscillations. Additionally, we plan to carry out a comprehensive analysis of the robustness of the system to fluctuations in parameters, quantification of the non-homogeneity of parameter values, and an investigation of stochastic effects such as noise in the system. We expect to report those results in a follow-up manuscript.

ACKNOWLEDGMENTS

We gratefully acknowledge support from the Office of Naval Research (ONR), Code 30. J.T., K.B., R.S., and A.P. were supported in part by National Science Foundation Grant No. CMMI-1068831 and by the Complex Dynamics and Systems Program of the Army Research Office, supervised by Dr. Samuel Stanton, under Grant No. W911NF-07-R-003-4. Also, we would like to acknowledge fruitful discussions with Professor M. Lakshmanan from Bharathidasan University, Professor Luciano Buono from the University of Ontario Institute of Technology, Professor Arkady Pikovsky and Professor Michael Rosenblum from the University of Potsdam, and Dr. Chitra Nayak from the University of Toronto.

¹I. Zutic, J. Fabian, and S. Sarma, "Spintronics: Fundamentals and applications," *Rev. Mod. Phys.* **76**, 323–410 (2004).

²L. Berger, "Emission of spin waves by a magnetic multilayer traversed by a current," *Phys. Rev. B* **54**(13), 9353–9358 (1996).

³J. C. Slonczewski, "Current-driven excitation of magnetic multilayers," *J. Magn. Magn. Mater.* **159**(13), L1–L7 (1996).

⁴V. Tiberkevich and A. Slavin, "Phase-locking and frustration in an array of nonlinear spin-torque nano-oscillators," *Appl. Phys. Lett.* **95**(26), 262505 (2009).

⁵A. E. Wickenden, C. Fazi, B. Huebschman, R. Kaul, A. C. Perrella, W. H. Rippard, and M. R. Pufall, "Spin torque nano oscillators as potential terahertz (THz) communications devices," Technical Report No. ARL-TR-4807, Army Research Laboratory, 2009.

⁶J. Grollier, V. Cros, and A. Fert, "Synchronization of spin-transfer oscillators driven by stimulated microwave currents," *Phys. Rev. B* **73**, 060409 (2006).

⁷S. Kaka, M. R. Pufall, W. H. Rippard, T. J. Silva, S. E. Russek, and J. A. Katine, "Mutual phase-locking of microwave spin torque nano-oscillators," *Nature* **437**(15), 389–392 (2005).

⁸J. Persson, Y. Zhou, and J. Akerman, "Phased-locked spin torque oscillators: Impact of device variability and time delay," *J. Appl. Phys.* **101**, 09A503 (2007).

⁹C. Serpico, R. Bonin, G. Bertotti, M. d'Aquino, and I. D. Mayergoyz, "Theory of injection locking for large magnetization motion in spin-transfer nano-oscillators," *IEEE Trans. Magn.* **45**(10), 3441–3444 (2009).

¹⁰W. H. Rippard, M. R. Pufall, S. Kaka, T. J. Silva, and S. E. Russek, "Injection locking and phase control of spin transfer nano-oscillators," *Phys. Rev. Lett.* **95**, 067203 (2005).

¹¹Z. Zeng, P. K. Amiri, I. N. Krivorotov, H. Zhao, G. Finocchio, J. P. Wang, J. A. Katine, Y. Huai, J. Langer, K. Galatsis, K. L. Wang, and H. W. Jiang, "High-power coherent microwave emission from magnetic tunnel junction nano-oscillators with perpendicular anisotropy," *ACS Nano* **6**(7), 6115–6121 (2012).

¹²D. Li, Y. Zhou, C. Zhou, and B. Hu, "Global attractors and the difficulty of synchronizing serial spin-torque oscillators," *Phys. Rev. B* **82**, 140407 (2010).

¹³J. M. Gambaudo, P. Glendinning, and C. Tresser, "The gluing bifurcation: I. Symbolic dynamics of the closed curves," *Nonlinearity* **1**, 203–214 (1988).

¹⁴M. Lakshmanan and K. Nakamura, "Landau-Lifshitz equation for ferromagnetism: Exact treatment of the Gilbert damping," *Phys. Rev. Lett.* **53**(26), 2497–2499 (1984).

¹⁵M. Lakshmanan, "The fascinating world of the Landau-Lifshitz-Gilbert equation: An overview," *Philos. Trans. R. Soc.* **369**, 1939, 1280–1300 (2011).

¹⁶G. Bertotti, I. D. Mayergoyz, and C. Serpico, "Analytical solutions of Landau-Lifshitz equation for precessional dynamics," *Physica B* **343**, 325–330 (2004).

¹⁷J. Z. Sun, "Spin-current interaction with a monodomain magnetic body: A model study," *Phys. Rev. B* **62**(1), 570–578 (2000).

¹⁸S. Muruges and M. Lakshmanan, "Spin-transfer torque induced reversal in magnetic domains," *Chaos, Solitons Fractals* **41**, 2773–2781 (2009).

¹⁹S. Muruges and M. Lakshmanan, "Bifurcation and chaos in spin-valve pillars in a periodic applied magnetic field," *Chaos* **19**, 043111 (2009).

²⁰E. Doedel and X. Wang, "Auto94: Software for continuation and bifurcation problems in ordinary differential equations," Applied Mathematics Report, California Institute of Technology, July 1994.

²¹A. S. Landsman and I. B. Schwartz, "Complete chaotic synchronization in mutually coupled time-delay systems," *Phys. Rev. E* **75**, 026201 (2007).

²²R. N. Chitra and V. C. Kuriakose, "Phase effects on synchronization by dynamical relaying in delay-coupled systems," *Chaos* **18**(2), 023129 (2008).

²³P. Hartman, *Ordinary Differential Equations*, 2nd ed. (Birkhauser, Boston, 1982).

²⁴A. Pikovsky, M. Rosenblum, and J. Kurths, *Synchronization: A Universal Concept in Nonlinear Sciences* (Cambridge University Press, 2001).

²⁵Y. Kuramoto, *Chemical Oscillations, Waves, and Turbulence* (Springer, Berlin, 1984).